Research paper

# Theoretical insights into the activation of $N_2O$ by a model Frustrated Lewis Pair. An ab-initio metadynamics study

Sebastián Gallardo-Fuentes[a], Rodrigo Ormazábal-Toledo[a,b,*]

[a] *Departamento de Química, Facultad de Ciencias, Universidad de Chile, Las Palmeras 3425, Casilla 653, Santiago, Chile*
[b] *Centro Integrativo de Biología y Química Aplicada (CIBQA), Universidad Bernardo OHiggins, Santiago 8370854, Chile*

## HIGHLIGHTS

- Activation of $N_2O$ mediated by FLPs occurs by the formation of an intermediate assited by a Lewis acid.
- Decomposition of FLP-$N_2O$ adduct is controlled by the rotation of P-N-N-O dihedral.
- Ab-initio metadynamics cogently describes the mechanism of activation of $N_2O$ by FLP.

## ARTICLE INFO

## ABSTRACT

Frustrated Lewis Pairs (FLPs) are a prominent class of substances capable of activation of small molecules. Albeit several experimental and theoretical studies devoted to the activation of greenhouse gases were recently published, activation of $N_2O$ are yet scarce. In present study we employed Density Functional Theory based metadynamics to reconstruct the Free Energy Landscape of the activation of $N_2O$ by the model $[t\text{-Bu}_3P][B(C_6F_5)_3]$ FLP. Similarly to the mechanism observed in the activation of $CO_2$, Lewis acid promotes the thermodynamic requirements of the reaction by stabilizing key intermediates. Regioselectivity of the activation of $N_2O$ as well as the effect of phosphine basicity are also discussed.

## 1. Introduction

Frustrated Lewis Pairs (FLPs) are a prominent class of acid-base pairs that have been widely used in catalysis [1–4]. FLPs are a special case of acid and base pairs in which steric congestion precludes the formation of a Lewis adduct [1,2,5]. For instance, the combination of different bulky substituted phosphines and boranes, as in $(C_6H_2Me_3)_2PH(C_6F_4)$ $BF(C_6F_5)_2$ salt, liberates $H_2$, at temperatures above 100 °C. Subsequent treatment with dihydrogen yields the original salt at room temperature [6]. The behavior encountered by Stephan and coworkers is normally attributed to the use of Lewis acids and Lewis bases where the steric demand *frustrates* the formation of the classical Lewis adduct. Just to mention a few notable applications of FLP chemistry are activation of $H_2$ [6,7]; binding of $CO_2$ [8,9], $SO_2$ [10], CO [11], NO [12], $N_2O$ [13], alkenes [14,15], alkynes [16] and dienes [17]. The role of FLPs as activating agents, has opened the possibility to activate greenhouse gases (GHG) as $CO_2$ [7–9]. The use of FLPs to activate other GHG as $N_2O$ are very scarce compared to $CO_2$ [13]. Even though $CO_2$ is the main responsible of global warming, $N_2O$

is not less harmful chemical. For instance, $N_2O$ remains in the atmosphere for more than 120 years having a global warming potential that is 300-fold greater than $CO_2$, mainly related to the catalytic destruction of atmospheric $O_3$ and high stability in the troposphere [18]. Different efforts have been made for sequestrating this GHG. For instance, one of the most used methods for its activation is promoted by transition metal catalysts [19,20] or N-heterocyclic carbenes [21,22]. Within the chemistry of FLPs the capture promoted by the $t\text{-Bu}_3P$ and $B(C_6F_5)_3$ was studied by Stephan and coworkers [13]. In their study, FLPs were allowed to react with $N_2O$ yielding the $t\text{-Bu}_3P\text{-NNO-}B(C_6F_5)_3$ adduct. By heating this compound, $N_2$ is liberated and formation of the Lewis acid-base adduct($t\text{-Bu}_3P = O$) $B(C_6F_5)_3$ was observed. Moreover, modifications on the FLP system by modifying the basicity of phosphine were unsuccessful. The only FLP that afforded $N_2O$ capture was $Cy_3P$ and $(C_6F_4\text{-}p\text{-H})_3$. However, the adduct $Cy_3P\text{-NNO-}(C_6F_4\text{-}p\text{-H})_3$ readily decomposed losing $N_2$ [13]. From a theoretical point of view, electronic and steric effects studies that promotes (or precludes) the activation of $N_2O$ are even scarcer. For instance, the formation of different complexes of $N_2O$ and several FLPs was computationally studied by Gilbert

* Corresponding author.
  *E-mail address:* rodrigo.ormazabal@ubo.cl (R. Ormazábal-Toledo).

[23]. The author point out that the capture of $N_2O$ is facilitated by the presence of acidic boranes that stabilizes electronic charge by increasing the charge over oxygen atom rather than nitrogen atom in $N_2O$. However, the question about the readily decomposition of $Cy_3P$ derivatives was unclear, and therefore still remains as an open question. More recently, Chattaraj and coworkers, studied the regioselectivity on the activation of $N_2O$ brought about by 1,4,2,5-diazadiborinine as FLP [24]. In this case, the most stable compound was related to an enhanced orbital contribution promoting the interaction between $N_2O$ and the intramolecular FLP. Different reports in the field of molecular dynamics concerning the chemistry of FLP were published by Privalov and coworkers [25,26]. In these works the activation of $H_2$ brought about by FLP was studied using Ab-Initio Molecular Dynamics describing the reaction mechanism in the gas phase and in the presence of explicit solvent. Rather recently, Pápai compared these works about the activation of $H_2$ by using static and dynamic models.[27] The role of FLP in the activation of $CO_2$ was also studied by Privalov by using molecular dynamics simulations [28]. In a similar way, Ensing and coworkers studied the activation of $H_2$[29] and $CO_2$[30] by using a density functional theory based Metadynamics simulations [31,32]. In the reaction of $CO_2$, the activating role of phosphine and stabilizing role of borane was unraveled by reconstructing the free energy surface [30]. Similarly, by studying the activation of $H_2$ the free energy landscape reveals that the reaction proceeds through the formation of a hydride and a protonated species in a single-step mechanism [29]. In this sense, the capture reaction of $N_2O$ promoted by FLPs appears as a system whose reaction mechanism remains unclear [23]. Moreover, the role that different phosphines presents in the activation mechanism needs a deeper analysis. In order to understand the role that a model FLP presents in the activation reaction of $N_2O$ the free energy landscape will be computed in order to assess the reaction mechanism of this process. In this sense, the working hypothesis establishes that it is possible to unravel the electronic and steric requirements that promotes the addition of $N_2O$ to a model FLP by using Metadynamics to reconstruct its free energy landscape. The article is organized as follows, in a first part, regioselectivity patterns on the activation of $N_2O$ by $t$-$Bu_3P$ and $B(C_6F_5)_3$ were studied by computing the free energy surface for three different modes of activation. Secondly, the activation of $N_2O$ promoted by two different FLPs was afforded to understand the role that phosphine presents in the reaction outcome.

## 2. Computational methods

An initial guess of FLP-$N_2O$ adduct was obtained at the HF/6-31G(d) level of theory. Geometry obtained was compared with cristallographic data available revealing similar trends in key bond distances and angles [13]. This geometry was then used for an equilibration in an NVT ensemble during 5 ps. After equilibration, metadynamics was used to reconstruct the free energy landscape [31,32]. In the metadynamics approach we used two collective variables, namely, the B-N or B-O coordination number and the P-N coordination number. The given coordination number was chosen based on the studied regioisomer. Tipically, $r_0$ values were 5.2 a.u. and 6.4 a.u. for P-N and B-O distances, respectively. The use of coordination number (CN) as collective variables has the advantage of describing the system in bounding ($s_{ij} = 1$) and an unbounding stage ($s_{ij} = 0$). In present case, the working formula for coordination number is

$$s_{ij} = \frac{\left(1 - \frac{r_{ij}}{r_0}\right)^{12}}{\left(1 - \frac{r_{ij}}{r_0}\right)^{24}}$$

(1)

In Eq. 1, $r_0$ is a parameter that describes each bond and $r_{ij}$ is the instantaneous distance between atoms $i$ and $j$. Quadratic walls with force constant $K = 0.01\,a.u.$ were used to avoid sampling irrelevant zones of the landscape. Particularly, B-P and B-N distances were restricted to be no more than $r_0 = 10$ bohr. In all cases the Gaussian bias potential was added every 25 steps, with a height of 0.25 kcal/mol and widths of 0.2 along the P-N and B-O CN and 0.1 a.u. along the P-$N_A$-$N_B$-O torsional angle. After 15 ps of metadynamics, Gaussian potential was added every 50 steps with a height of 0.10 kcal/mol until the surface was completely reconstructed (normally within 40 ps). All dynamical simulations were performed with the Quickstep module of CP2K version 6.0 by using the GPW method [33]. The valence orbitals were expanded in the DZVP-MOLOPT-SR-GTH basis set [34–36], while an auxiliary plane-wave basis set up to the kinetic energy cutoff of 250 Ry was used to describe valence electron density. Core electrons were replaced by pseudopotential. The PBE augmented with Grimme D3 disperison correction was used along the simulations.[37,38] A rather large simulation box of $20 \times 20 \times 20$ Å together with a global chain Nosé-Hoover thermostat of length 4 was used to maintain the system at 300 K. In all cases, MD time step was set up to 0.5 fs. Static calculations were performed with Gaussian 09 using the LC-$\omega$PBE/6-31 + G(d,p) level of theory.[39] Natural population analysis as well as Fukui function were obtained using procedures reported elsewhere.[40–42]

## 3. Results

### 3.1. Origin of the regioselectivity on the $N_2O$ addition to $t$-$Bu_3P$–$B(C_6F_5)_3$ FLP.

Firstly, we computed the free energy landscape associated with the addition of $[t$-$Bu_3P][B(C_6F_5)_3]$ FLP to $N_2O$. As proposed by Chattaraj and coworkers, different adducts may be obtained in the addition reaction of 1,4,2,5-diazadiborinine to $N_2O$, where two boron atoms are the Lewis acid and basic centers.[24] However, the authors suggest that the main product should be that obtained with O and external N in $N_2O$ interacting with the boron atoms. Moreover, according to Gilbert a set of 5 regioisomers should be obtained in the reaction.[23] In the present work we just analyzed those three regioisomers with less steric congestion as shown in Fig. 1b-d labelled as **1A**, **1B** and **1C**.

The reaction mechanism was studied starting from the bounded state of the adducts. As suggested previously by Ensing and coworkers, the FLP-gas adduct is a rigid structure that facilitates the metadynamics computation by studying a problem of a single molecule ($t$-$Bu_3P$-NNO-B$(C_6F_5)_3$ complex) rather than a problem of 3 unbounded molecules.[30] Therefore, in the course of the AIMD simulation we first computed the expulsion of $N_2O$ followed by the acid-base interaction of $B(C_6F_5)_3$ and $t$-$Bu_3P$. In contrast to $CO_2$ capture by $B(C_6F_5)_3$ and $t$-$Bu_3P$ FLP, the reaction mechanism of the activation of $N_2O$ remains unclear. Present computations reveal that depending on the type of approximation of $N_2O$, different mechanism may be proposed. Fig. 2 displays free energy surfaces for each reaction obtained from AIMD Metadynamics. Additionally, Fig. 3 presents structures of the minima obtained in each surface on Fig. 2.
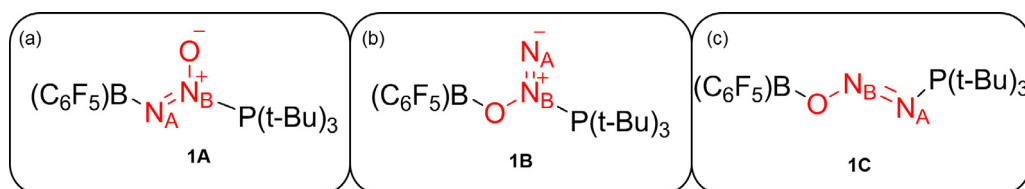


**Fig. 1.** Regioisomers considered in present study: (a) **1A**, (b) **1B** and (c) **1C**.
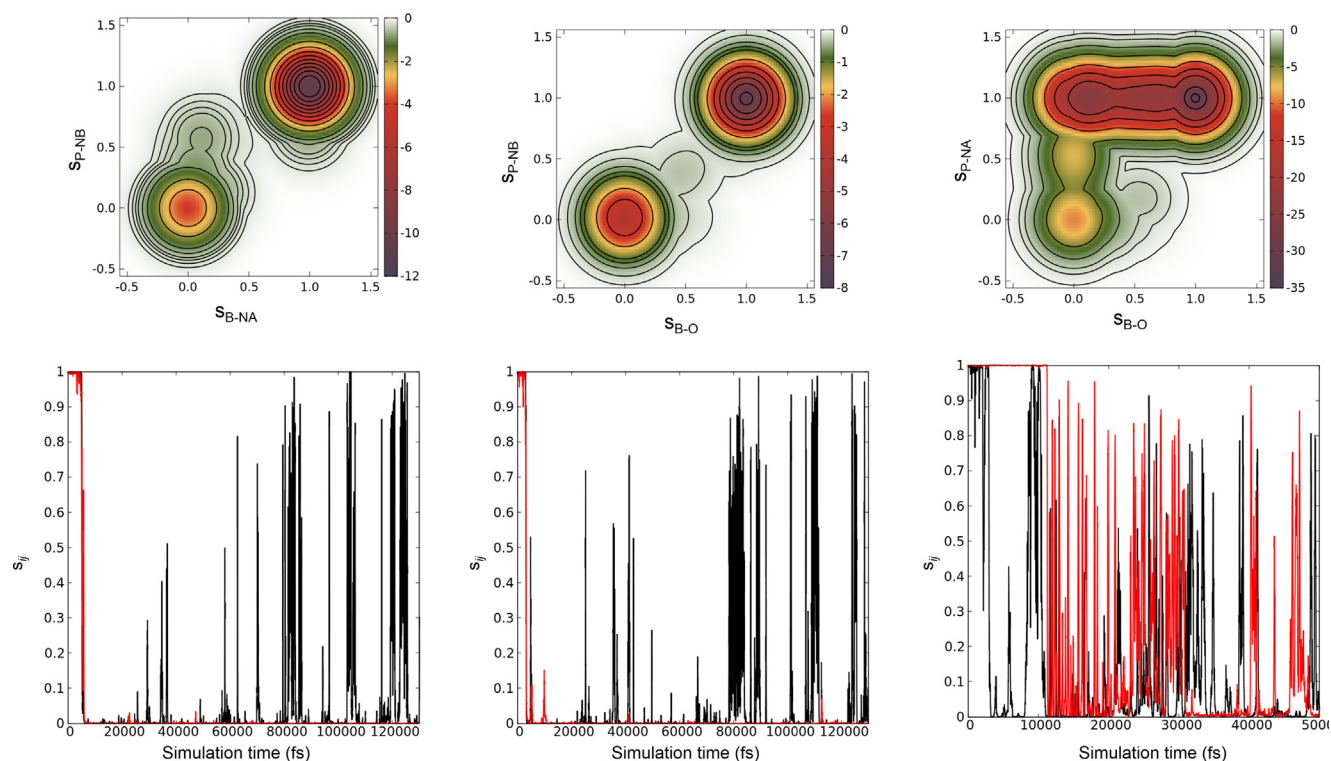
**Fig. 2.** (a) Smoothed free energy surface (in kcal/mol) for the formation of adducts **1A** (isolines are presented every 1 kcal/mol), **1B** (isolines are presented every 1 kcal/mol) and **1C** (isolines are presented every 2 kcal/mol). Raw free energy profiles were included in Supporting Information. (b) Variation of $s_{ij}$ collective variable along the simulation time.

Note that for the reaction of formation of **1A**, computations predict a single step, but highly asynchronous mechanism, passing through $s_{ij} = 0.5$ within similar times as shown in Fig. 2b. Energetics for this reaction are $\Delta F^{\ddagger} = 3.6$ kcal/mol and $\Delta F^0 = 7.0$ kcal/mol. In the case of

formation of adduct **1B**, the mechanism is also single step, but revealing a more synchronous association. In this case, activation and reaction free energy barriers are $\Delta F^{\ddagger} = 3.5$ kcal/mol and $\Delta F^0 = 3.3$ kcal/mol, respectively. Finally, for product **1C**, computations reveal a two-step
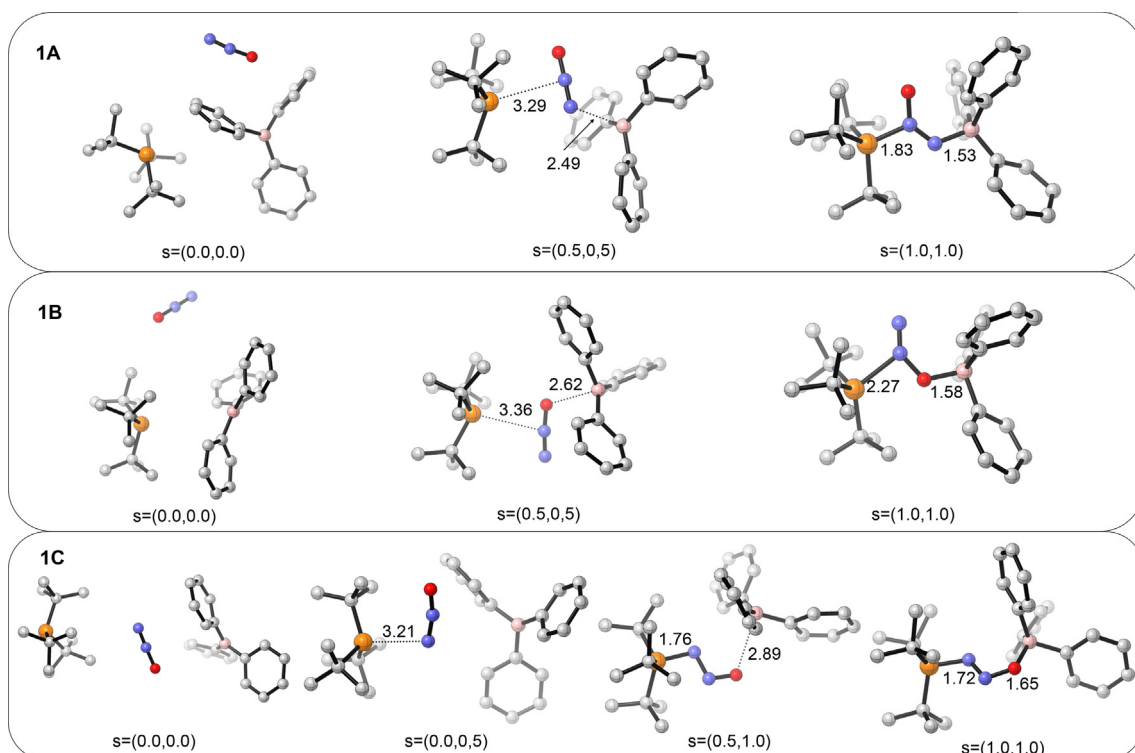


**Fig. 3.** Structures of the minima obtained during the Metadynamic simulation of **1A**, **1B** and **1C**. Hydrogen and fluorine atoms were omitted for clarity.
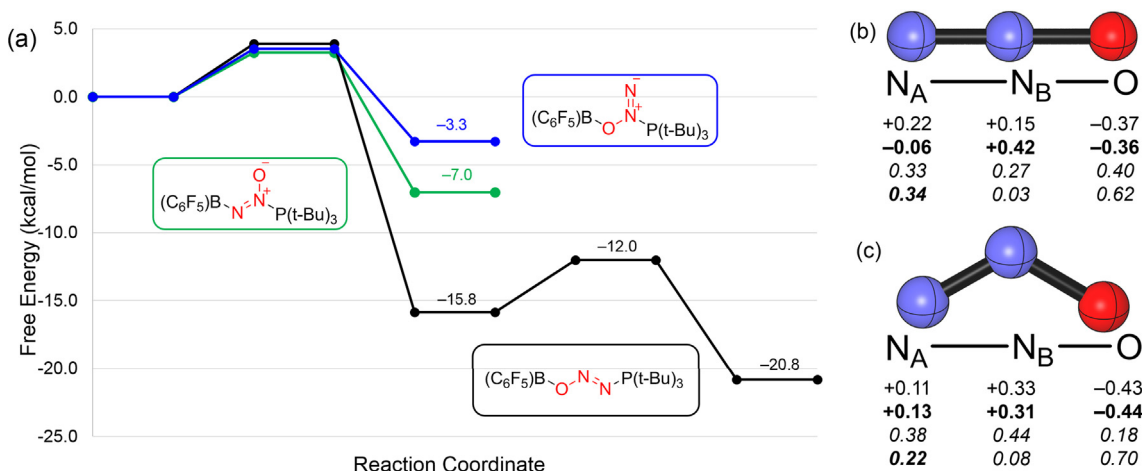
**Fig. 4.** (a): Free energy ($\Delta F$) profiles for the formation of adducts **1A** (green), **1B** (blue) and **1C** (black). (b) and (c): atomic charges computed within the AIM (plain text) and NBO (bold text) schemes and the electrophilic (italic text) and nucleophilic (italic and bold text) Fukui functions for $N_2O$ in two geometries. (For interpretation of the references to colour in this figure legend, the reader is referred to the web version of this article.)
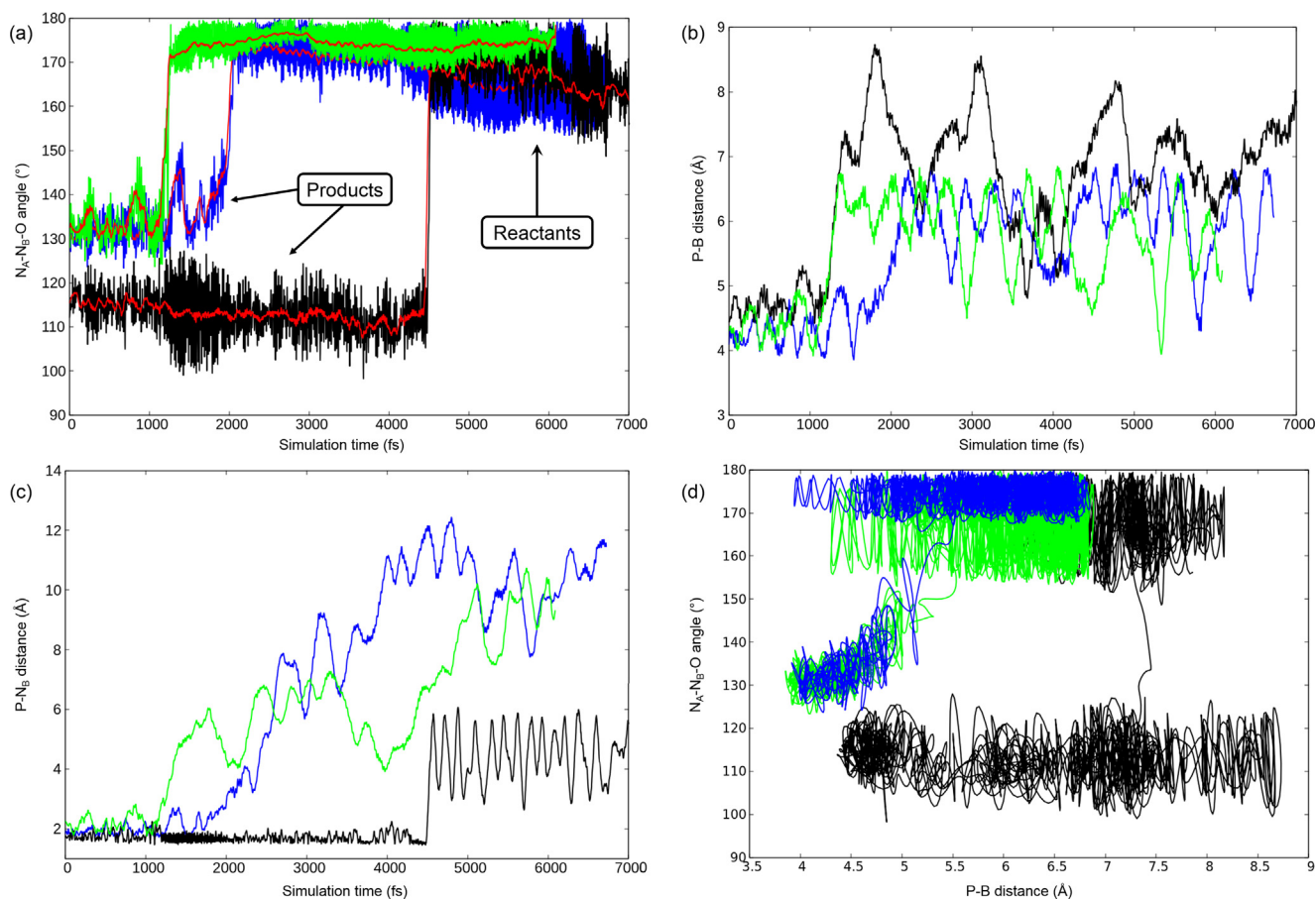


**Fig. 5.** Variation along the simulation time (in fs) of (a) $N_A$-$N_B$-O angle, (b) P atom (in phosphine) and B atom (in borane) distance, (c) P atom (in phosphine) and $N_B$ atom of $N_2O$. (d) Variation of P-B and P-$N_B$ distance within the first 1000 fs where the $t$-Bu$_3$P-NNO-B(C$_6$F$_5$)$_3$ complex is formed. Color code is as follows: green: **1A**, blue: **1B**, black: **1C**, red: mean value of $N_A$-$N_B$-O angle.

mechanism being the first step the nucleophilic attack of phosphine, followed by a stabilization of the oxyanion formed by the Lewis acid (see 2b, reminiscent to the mechanism of activation of $CO_2$ [30,43]. In this case, barriers relative to reactants are as follow: $\Delta F^{\ddagger} = 3.9$ kcal/mol and $\Delta F^0 = 20.8$ kcal/mol. Fig. 4a shows the one-dimension free energy profile for the formation of each adduct.

Computed energetics for these systems present quite similar and low activation energies compared to the activation of $CO_2$ [30]. However,

these results are in good agreement with the experimental observations [13]. Albeit the three reaction mechanisms computed display similar activation free energies, the main differences were observed in the reaction energies displayed in Fig. 4a, where **1C** is the most stable adduct obtained. To give deeper insights about the formation of different adducts, an electronic analysis on the $N_2O$ fragment was performed. Linear and bend configurations of $N_2O$ were chosen from the simulation and then removing the Lewis pair. In this sense, angular and linear

configurations were taken from the first and the last snapshots of the simulation, respectively. The results are presented in Fig. 4b and 4c. Atomic charges were obtained within the Natural Population Analysis (NPA) approach [40]. Moreover, electrophilic and nucleophilic Fukui functions were calculated by using a methodology proposed elsewhere [41,42]. The NPA analysis reveals that oxygen presents the most negative charges and central nitrogen ($N_B$) is the most positive. This result may be traced to the different trend of each atom towards a nucleophilic attack (by phosphine) and a subsequent association with B $(C_6F_5)_3$, that may be related to an electrophilic displacement. Hence, oxygen in any case should not be attacked by phosphine and, according to its atomic charge, it may be stabilized by borane after nucleophilic attack. On the other hand, the values obtained for the condensed to atoms Fukui Function reveals a nucleophilic reactivity at the oxygen atom and a higher electrophilic reactivity at the $N_A$ atom [41]. These results highlight that the origin of the regioselectivity observed for the formation of **1B** may be related to a frontier molecular orbital controlled mechanism rather than a charge controlled mechanism. As reported previously by part of us, nucleophilic Fukui function may asses the electrofugality patterns of a fragment after the nucleophilic attack (see Fig. 4c).[44] Again, the results suggest that oxygen should stabilize the electronic charge assisted by borane. Moreover, in the bend configuration of $N_2O$, $N_B$ turns into an electrophilic center. However, its reactivity may be precluded by the steric congestion induced by Lewis acid and base pairs related to a higher distortion energy. In this sense, the repulsive steric interaction arises from the overlap between closed-shell orbitals of these isotropically bulky groups. In this line, steric congestion is a key feature in FLP chemistry that should be considered. For this reason, a geometrical analysis based on the results obtained along the simulation was performed. They are presented in Fig. 5, below.

By considering Fig. 5a, the variation of $N_A$-$N_B$-O angle along the simulation time reveals an interesting response in the formation of adduct **1C** respect to **1A** or **1B**. Note that at the reactants stage, $N_2O$ displays a quasilinear geometry presenting a $N_A$-$N_B$-O angle near $170°$ for the three systems. However, in the bent configuration of $N_2O$, different values may be obtained, depending on the regioisomer observed. Then, for **1A** and **1B**, the $N_A$-$N_B$-O angle is within the range of $130–140°$, while for **1C** the observed angle is $115°$. In line with the activation strain model, the most distorted system should produce the most interacting pair as proposed by Houk and Bickelhaupt in a model $S_N2$ reaction [45]. In a qualitative fashion, the higher stability of adduct **1C** may be related to the higher distortion of the $N_A$-$N_B$-O angle. Similarly, for $CO_2$ activation promoted by ionic liquids, the bent configuration of $CO_2$ (high distortion) was previously related with a higher reactivity of the system based on quantum mechanical calculations.[43] Hence, adducts **1A** and **1B** should be less stable than **1C** due to their negligible distortion energy and consequently, a lower interaction energy (in the **1A** and **1B** adducts). Moreover, Fig. 5b shows that the distance between phosphine and borane moieties (represented as the P-B distance for the sake of simplicity) is larger in the formation of adduct **1C** than in **1A** or **1B**. The geometry observed for **1A** and **1B** in Fig. 1, requires shorter P-B distance, enhancing the acid-base steric congestion, thereby precluding the formation of a stable adduct. Similarly, distance between phosphorous and N attacked in the region of products formation reveals that for **1C**, $N_A$ and P bond is shorter than $N_B$-P in **1A** and **1B** (see Fig. 1). These results may strongly be related to activation strain model since the most distorted system (higher $N_A$-$N_B$-O angle and shorter $N_A$-P distance) is the most stable due to its higher interaction energy. Fig. 5d reveals another interesting feature of these adducts by comparing the $N_A$-$N_B$-O angle and the P-B distance. For adducts **1A** and **1B**, shorter P-B distances are needed for the activation of $N_2O$, while for **1C** even at larger P-B distances $N_2O$ presents a bent configuration. This result must be related with the free energy landscape presented in Fig. 1. For **1A** and **1B** the reaction mechanism is single step, that is, phosphine and borane react with $N_2O$ in the same step of the reaction.

On the other hand, for the formation of adduct **1C** phosphine attacks $N_2O$ and borane stabilizes the intermediate formed in a second step. Similarly to the chemistry of activation of $CO_2$, the formation of a bent $N_2O$ may be driven with a highly nucleophilic phosphine (or other nucleophile) without the assistance of a Lewis acid. In this sense, the use of a highly acidic borane allows the isolation of a stable adduct, however, if it needed the formation of a reactive $N_2O$ intermediate (namely, in a tandem reaction), the use of Lewis acid should be avoided.

### 3.2. Effects of change phosphine basicity on the properties of FLP in the reaction towards $N_2O$.

Experimental and theoretical studies suggest that different phosphines may be used as Lewis bases for studying the activation of $N_2O$ [13]. However, only $(t$-Bu$)_3$P yields a stable product. By using other less basic phosphines no products were observed. One of the few affordable phosphines is $Cy_3P$, nevertheless, the adduct observed quickly collapses forming $N_2$ gaseous and phosphine oxide. Similarly, by heating the $t$-Bu$_3$P-NNO-B$(C_6F_5)_3$ adduct, $N_2$ and phosphine oxide was obtained [13]. One reason to this response was related to the feasibility of the rotation of the adduct, as presented in Fig. 6a, where adduct obtained during the simulation was forced to rotate for analyzing the P-$N_A$-$N_B$-O torsional angle.

The free energy landscape for the torsion of the P-$N_A$-$N_B$-O dihedral was obtained by using a similar metadynamic simulation as described above for $t$-Bu$_3$P-NNO-B$(C_6F_5)_3$ (**1C**, black) and $Cy_3$P-NNO-B$(C_6F_5)_3$ (**1D**, red) adducts (see Fig. 6b). For *trans*-**1C**, the activation free energy for rotation is $\Delta F^{\ddagger} = 12.1$ kcal/mol. The *cis*-**1C** complex obtained is located 0.7 kcal/mol above the *trans*-**1C** isomer. While both stereoisomers present similar reaction energetics, the activation energy precludes the interconversion of both isomers at room temperature. On the other hand, for **1D** only the *cis* isomer was observed after a long simulation time as shown in Fig. 6c. Indeed, the minimum on its free energy profile, is always located near a P-$N_A$-$N_B$-O torsional angle of $80°$. In contrast, for **1C** torsional angle presents two minima located at $162°$ (*trans*-**1C**) and $5°$ (*cis*-**1C**). In order to assess different reactivity patterns observed in **1C** respect to **1D**, an additional analysis over the metadynamic simulation was performed. The results are displayed in Fig. 7 highlighting the variation of $N_A$-$N_B$-O angle along the simulation. Since the computation of system **1D** was near 20 times longer than **1C**, only the first part of its simulation is presented in Fig. 7.

In both cases, at the beginning of the simulation, the system remains in the *cis* isomer. However, after a short time **1C** bents from $120°$ to $110°$ by passing from *cis* to *trans* stereoisomer. As discussed above, this situation favors the interaction between $N_2O$ and the Lewis acid and base pair. On the other hand, for **1D**, the system is always located in the *cis* geometry with higher $N_A$-$N_B$-O angle (near $120°$), thereby unraveling that this configuration may be unstable. According to experimental reports by Stephan, the $Cy_3$P-NNO-B$(C_6F_5)_3$ as well as $t$-Bu$_3$P-NNO-B$(C_6F_5)_3$ adducts would decompose affording gaseous $N_2$ and phosphine oxide.[13] Fig. 7b presents the variation of $N_A$-$N_B$-O angle vs. P-$N_A$-$N_B$-O dihedral. Note that at higher dihedral values, shorter $N_A$-$N_B$-O angles are observed, revealing the stabilizing role of the Lewis base. In this sense, the rotation along the P-$N_A$-$N_B$-O dihedral promotes the stabilization of the FLP-$N_2O$ adduct. A deeper analysis on the reaction trajectory obtained in the metadynamic simulations, would give several insights about the decomposition process. Fig. 8a and b display the variations of $N_A$-$N_B$ and P-O distance.

The bond distances analyzed were chosen considering that in the expulsion of $N_2$, a $N_A$-$N_B$ bond shortening should be observed. Moreover, if phosphine oxide is formed, P-O bond would also be shorter. As shown in Fig. 8a, in the *cis* configuration of both adducts the $N_A$-$N_B$ distance is quite similar, however, as time goes and **1C** adduct rotates to its *trans* isomer the bond is clearly elongated. This result suggests that in the *cis* configuration, the system could release $N_2$ easier
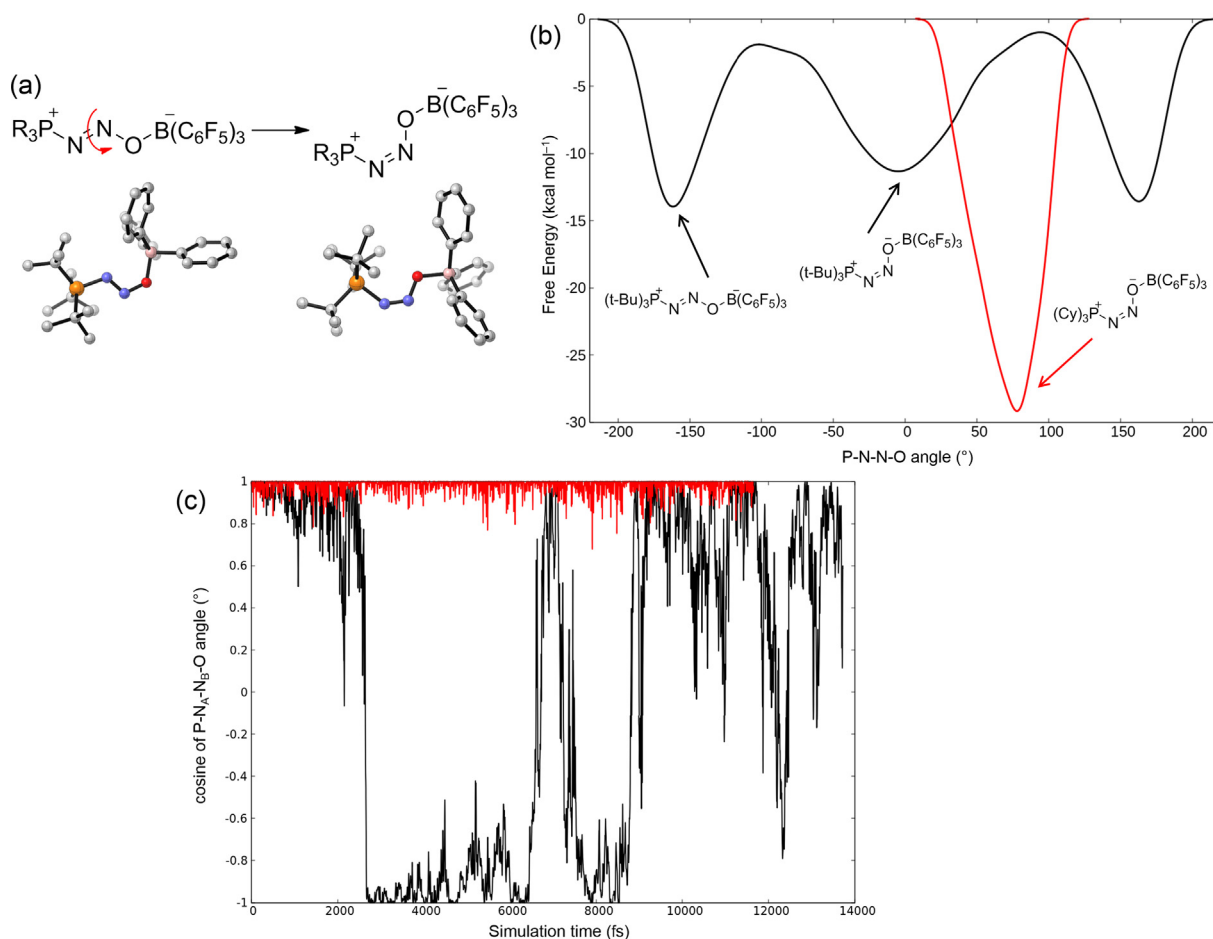
**Fig. 6.** (a) Rotation of P-$N_A$-$N_B$-O dihedral angle. Hydrogen and fluorine atoms were omitted for simplicity. (b) Free energy profile for the rotation of P-$N_A$-$N_B$-O dihedral angle in *t*-Bu$_3$P-NNO-B(C$_6$F$_5$)$_3$ (black) and Cy$_3$P-NNO-B(C$_6$F$_5$)$_3$ (red). (c) Variation of P-$N_A$-$N_B$-O dihedral during the simulation.

than in the *trans* region. Moreover, Fig. 8b reveals that in **1D** P-O distance is shorter than *cis*-**1C** or *trans*-**1C** along the simulation. Hence, **1D** should decompose easier than **1C** as reported elsewhere.[13] Fig. 8c shows a typical configuration of *cis*-**1C** and *cis*-**1D** revealing that P-O distance is shorter in the former. This response may be related to steric congestion of the *t*-Bu moieties that repeals the C$_6$F$_5$ groups in borane. In **1D**, phosphine is substituted by three cyclohexyl fragments presenting a secondary carbon atom. This difference may be responsible of

an enhanced acid base repulsion in **1C** allowing a higher P-O distance. Finally, Fig. 8d displays a plausible reaction mechanism for this step based on the outcomes of this metadynamic. The mechanism consists of an electrocyclic-like transition state where oxygen atom attacks the positively charged phosphonium moiety promoting the expulsion of gaseous N$_2$ and the formation of phosphine oxide. This mechanism is just a proposal and was not confirmed by any quantum mechanical computation because it is out of the scope of the article.
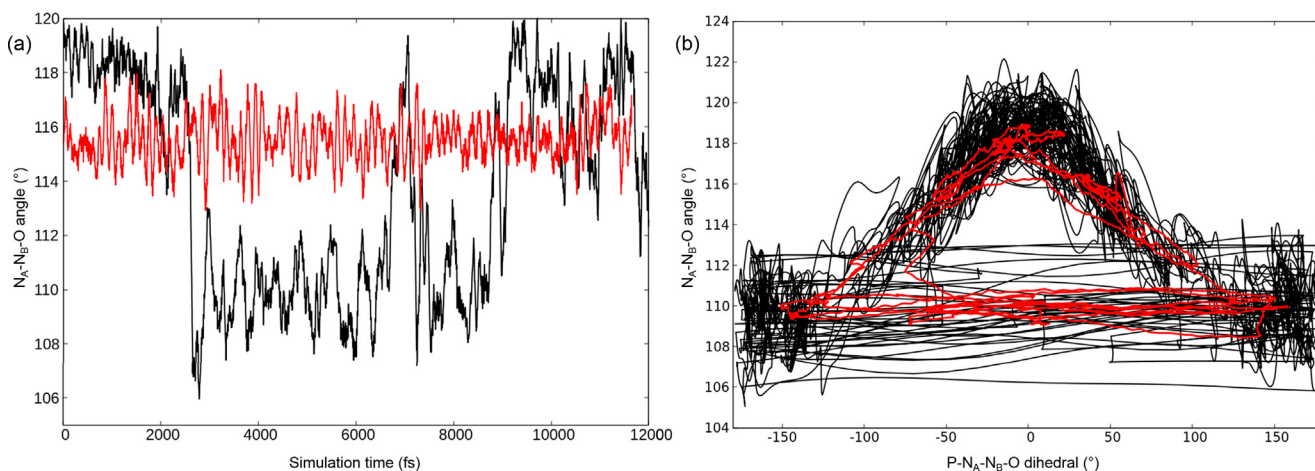




**Fig. 7.** (a) Variation of $N_A$-$N_B$-O angle (in degrees) along the simulation time (in fs) for the simulation of *t*-Bu$_3$P-NNO-B(C$_6$F$_5$)$_3$ (black) and Cy$_3$P-NNO-B(C$_6$F$_5$)$_3$ (red). (b) Variation of $N_A$-$N_B$-O angle vs. P-$N_A$-$N_B$-O dihedral for the simulation of *t*-Bu$_3$P-NNO-B(C$_6$F$_5$)$_3$ (black) and its mean value (red). (For interpretation of the references to colour in this figure legend, the reader is referred to the web version of this article.)
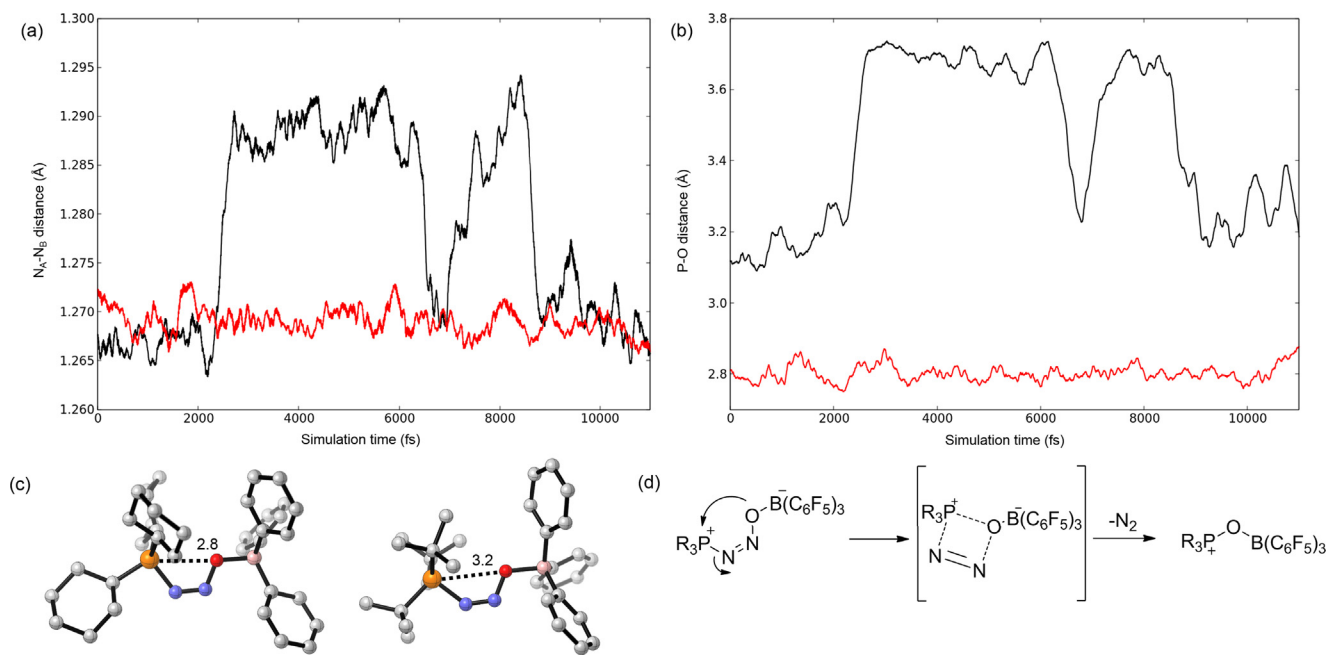
**Fig. 8.** Variation of (a) $N_A$-$N_B$ distance and (b) P-O distance along the simulation time. (c) Typical *cis*-**1C** and *cis*-**1D** geometries obtained in the final step of the simulation. Distances are in Å. (d) Plausible reaction mechanism for the expulsion of $N_2$ and formation of phosphine oxide.

## 4. Concluding remarks

In summary, the activation of $N_2O$ brought about by the model [*t*-Bu$_3$P][B(C$_6$F$_5$)$_3$] FLP was computed by means of Density Functional Theory based Metadynamics. This approach allows to reconstruct the reaction pathway for the formation of the *t*-Bu$_3$P-NNO-B(C$_6$F$_5$)$_3$ adduct. Regioselectivity of the reaction shows that adduct **1C** is the preferred one in line with experimental results. Other adducts may be observed, however, they are thermodynamically less favored. The higher stability observed for adduct **1C** is related to two main factors: (i) a more distortion of $N_2O$ fragment promoted by the Lewis acid, and (ii) a lesser steric congestion due to a higher phosphine-borane distance. Results obtained suggests that the formation of adduct **1C** requires less electronic demand due to a higher electrophilic activation of terminal N atom. The role of phosphine basicity was also discussed in terms of the rotation of the P-$N_A$-$N_B$-O torsional angle. In this sense, albeit less basic phosphine as Cy$_3$P could form the Cy$_3$P-NNO-B(C$_6$F$_5$)$_3$ adduct, its geometry (a *cis*-like derivative) allows the decomposition into $N_2$ and phosphine oxide in contrast to the *trans*-like derivative observed for **1D**. These results highlight the role of phosphine in the activation of $N_2O$ and, moreover, suggests the ability of Lewis acid for stabilizing the adduct formed in the reaction.

## Declaration of Competing Interest

The authors declare that they have no known competing financial interests or personal relationships that could have appeared to influence the work reported in this paper.

## Acknowledgements

## Appendix A. Supplementary material

Supplementary data associated with this article can be found, in the online version, at https://doi.org/10.1016/j.cplett.2019.137002.

## References

[1] D. Stephan, G. Erker, Frustrated lewis pair chemistry: development and perspectives, Angew. Chem. Int. Ed. 54 (22) (2015) 6400–6441.

[2] D. Stephan, Frustrated lewis pairs: from concept to catalysis, ACC. Chem. Res 48 (2) (2015) 306–316.

[3] D. Stephan, Frustrated lewis pairs, J. Am. Chem. Soc. 137 (32) (2015) 10018–10032.

[4] D. Stephan, Frustrated lewis pairs: a new strategy to small molecule activation and hydrogenation catalysis, Dalton Trans. 17 (2009) 3129–3136.

[5] D. Stephan, G. Erker, Frustrated lewis pairs: metal-free hydrogen activation and more, Angew. Chem. Int. Ed. 49 (1) (2010) 46–76.

[6] G.C. Welch, R.R.S. Juan, J.D. Masuda, D.W. Stephan, Reversible, metal-free hydrogen activation, Science 314 (5802) (2006) 1124–1126.

[7] D.W. Stephan, Frustrated lewis pairs, J. Am. Chem. Soc. 137 (32) (2015) 10018–10032.

[8] C. Mömming, E. Otten, G. Kehr, R. Fröhlich, S. Grimme, D. Stephan, G. Erker, Reversible metal-free carbon dioxide binding by frustrated lewis pairs, Angew. Chem. Int. Ed. 48 (36) (2009) 6643–6646.

[9] I. Peuser, et al., Co2 and formate complexes of phosphine/borane frustrated lewis pairs, Chem. Eur. J. 17 (35) (2011) 9640–9650.

[10] D.W. Stephan, G. Erker, Frustrated lewis pair chemistry of carbon, nitrogen and sulfur oxides, Chem. Sci. 5 (2014) 2625–2641.

[11] M. Sajid, L.-M. Elmer, C. Rosorius, C.G. Daniliuc, S. Grimme, G. Kehr, G. Erker, Facile carbon monoxide reduction at intramolecular frustrated phosphane/borane lewis pair templates, Angew. Chem. Int. Ed. 52 (8) (2013) 2243–2246.

[12] A.J.P. Cardenas, et al., Capture of no by a frustrated lewis pair: a new type of persistent n-oxyl radical, Angew. Chem. Int. Ed. 50 (33) (2011) 7567–7571.

[13] E. Otten, R.C. Neu, D.W. Stephan, Complexation of nitrous oxide by frustrated lewis pairs, J. Am. Chem. Soc. 131 (29) (2009) 9918–9919.

[14] X. Zhao, D.W. Stephan, Olefinborane van der waals complexes: intermediates in frustrated lewis pair addition reactions, J. Am. Chem. Soc 133 (32) (2011) 12448–12450.

[15] Y. Guo, S. Li, A novel addition mechanism for the reaction of frustrated lewis pairs with olefins, Eur. J. Inorg. Chem. 2008 (16) (2008) 2501–2505.

[16] X. Zhao, A.J. Lough, D.W. Stephan, Synthesis and reactivity of alkynyl-linked phosphonium borates, Chem. Eur. J. 17 (24) (2011) 6731–6743.

[17] M. Ullrich, K.S.-H. Seto, A.J. Lough, D.W. Stephan, 1,4-addition reactions of frustrated lewis pairs to 1,3-dienes, Chem. Commun. 2335–2337 (2009).

[18] B. Bates, Z. Kundzewicz, S. Wu, Climate Change and Water, Intergovernmental Panel on Climate, Change Secretariat, 2008.

[19] W. Tolman, Binding and activation of n2o at transition-metal centers: recent mechanistic insights, Angew. Chem. Int. Ed. 49 (6) (2010) 1018–1024.

[20] E. Poulain, A. Rubio-Ponce, V.H. Uc, V. Bertin, O. Olvera-Neria, Importance of pd

and pt excited states in n2o capture and activation: a comparative study with rh and au atoms, Int. J. Quantum Chem. 113 (13) (2013) 1794–1802.

[21] A.G. Tskhovrebov, E. Solari, M.D. Wodrich, R. Scopelliti, K. Severin, Covalent capture of nitrous oxide by n-heterocyclic carbenes, Angew. Chem. Int. Ed. 51 (1) (2012) 232–234.

[22] L.Y.M. Eymann, R. Scopelliti, F.T. Fadaei, G. Cecot, E. Solari, K. Severin, Fixation of nitrous oxide by mesoionic and carbanionic n-heterocyclic carbenes, Chem. Commun. 53 (2017) 4331–4334.

[23] T.M. Gilbert, Computational studies of complexation of nitrous oxide by borane phosphine frustrated lewis pairs, Dalton Trans. 41 (2012) 9046–9055.

[24] M. Ghara, P.K. Chattaraj, Fixation of nitrous oxide (n2o) by 1, 4, 2, 5-diazadiborinine: a dft study, Int. J. Quantum Chem. 118 (14) (2018) e25593.

[25] M. Pu, T. Privalov, Ab initio molecular dynamics with explicit solvent reveals a two-step pathway in the frustrated lewis pair reaction, Chem. Eur. J. 21 (49) (2015) 17708–17720.

[26] M. Pu, T. Privalov, Uncovering the role of intra- and intermolecular motion in frustrated lewis acid/base chemistry: ab initio molecular dynamics study of co2 binding by phosphorus/boron frustrated lewis pair [tbu3p/b(c6f5)3], Inorg. Chem. 53 (9) (2014) 4598–4609.

[27] J. Daru, I. Bakó, A. Stirling, I. Pápai, Mechanism of heterolytic hydrogen splitting by frustrated lewis pairs: comparison of static and dynamic models, ACS Catal. 9 (7) (2019) 6049–6057.

[28] M. Pu, T. Privalov, How frustrated lewis acid/base systems pass through transition-state regions: H2 cleavage by [tbu3p/b(c6f5)3], ChemPhysChem 15 (14) 2936–2944.

[29] L. Liu, B. Lukose, B. Ensing, Hydrogen activation by frustrated lewis pairs revisited by metadynamics simulations, J. Phys. Chem. C 121 (4) (2017) 2046–2051.

[30] L. Liu, B. Lukose, B. Ensing, A free energy landscape of CO2 capture by frustrated lewis pairs, ACS Catal. 8 (4) (2018) 3376–3381.

[31] A. Laio, M. Parrinello, Escaping free-energy minima, Proc. Natl. Acad. Sci. U.S.A. 99 (20) (2002) 12562–12566.

[32] A. Barducci, M. Bonomi, M. Parrinello, Metadynamics, WIREs Comput. Mol. Sci. 1 (5) (2011) 826–843.

[33] J. Hutter, M. Iannuzzi, F. Schiffmann, J. VandeVondele, cp2k: atomistic simulations of condensed matter systems, WIREs Comput. Mol. Sci. 4 (1) (2014) 15–25.

[34] J. VandeVondele, J. Hutter, Gaussian basis sets for accurate calculations on molecular systems in gas and condensed phases, J. Chem. Phys. 127 (11) (2007) 114105.

[35] C. Hartwigsen, S. Goedecker, J. Hutter, Relativistic separable dual-space gaussian pseudopotentials from h to rn, Phys. Rev. B 58 (1998) 3641–3662.

[36] M. Krack, Pseudopotentials for h to kr optimized for gradient-corrected exchange-correlation functionals, Theor. Chem. Acc. 114 (1) (2005) 145–152.

[37] S. Grimme, S. Ehrlich, L. Goerigk, Effect of the damping function in dispersion corrected density functional theory, J. Comput. Chem. 32 (7) (2011) 1456–1465.

[38] S. Grimme, J. Antony, S. Ehrlich, H. Krieg, A consistent and accurate ab initio parametrization of density functional dispersion correction (dft-d) for the 94 elements h-pu, J. Chem. Phys. 132 (15) (2010) 154104.

[39] M.J. Frisch, G.W. Trucks, H.B. Schlegel, G.E. Scuseria, M.A. Robb, J.R. Cheeseman, G. Scalmani, V. Barone, G.A. Petersson, H. Nakatsuji, X. Li, M. Caricato, A.V. Marenich, J. Bloino, B.G. Janesko, R. Gomperts, B. Mennucci, H.P. Hratchian, J.V. Ortiz, A.F. Izmaylov, J.L. Sonnenberg, D. Williams-Young, F. Ding, F. Lipparini, F. Egidi, J. Goings, B. Peng, A. Petrone, T. Henderson, D. Ranasinghe, V.G. Zakrzewski, J. Gao, N. Rega, G. Zheng, W. Liang, M. Hada, M. Ehara, K. Toyota, R. Fukuda, J. Hasegawa, M. Ishida, T. Nakajima, Y. Honda, O. Kitao, H. Nakai, T. Vreven, K. Throssell, J.A. Montgomery, Jr., J.E. Peralta, F. Ogliaro, M.J. Bearpark, J.J. Heyd, E.N. Brothers, K.N. Kudin, V.N. Staroverov, T.A. Keith, R. Kobayashi, J. Normand, K. Raghavachari, A.P. Rendell, J.C. Burant, S.S. Iyengar, J. Tomasi, M. Cossi, J.M. Millam, M. Klene, C. Adamo, R. Cammi, J.W. Ochterski, R.L. Martin, K. Morokuma, O. Farkas, J.B. Foresman, D.J. Fox, Gaussian 09 Revision D.01, gaussian Inc. Wallingford CT (2016).

[40] A.E. Reed, R.B. Weinstock, F. Weinhold, Natural population analysis, J. Chem. Phys. 83 (2) (1985) 735–746, https://doi.org/10.1063/1.449486.

[41] R.R. Contreras, P. Fuentealba, M. Galvn, P. Prez, A direct evaluation of regional fukui functions in molecules, Chem. Phys. Lett. 304 (5) (1999) 405–413.

[42] P. Fuentealba, P. Prez, R. Contreras, On the condensed fukui function, J. Chem. Phys. 113 (7) (2000) 2544–2551.

[43] S. Gallardo-Fuentes, R. Contreras, M. Isaacs, J. Honores, D. Quezada, E. Landaeta, R. Ormazábal-Toledo, On the mechanism of CO2 electro-cycloaddition to propylene oxides, J. CO2 Util. 16 (2016) 114–120.

[44] R. Ormazábal-Toledo, P.R. Campodónico, R. Contreras, Are electrophilicity and electrofugality related concepts? a density functional theory study, Org. Lett. 13 (4) (2011) 822–824.

[45] F.M. Bickelhaupt, K.N. Houk, Analyzing reaction rates with the distortion/inter-action-activation strain model, Angew. Chem. Int. Ed. 56 (34) (2017) 10070–10086.